

The cortical deficit in humans with strabismic amblyopia

G. R. Barnes, R. F. Hess, S. O. Dumoulin, R. L. Achtman and G. B. Pike*

*McGill Vision Research, Department of Ophthalmology, McGill University,
and *McConnell Brain Imaging Centre, Montreal Neurological Institute,
Montreal, Canada*

(Received 21 August 2000; accepted after revision 10 January 2001)

1. To further our understanding of the cortical deficit in strabismic amblyopia, we measured, compared and mapped functional magnetic resonance imaging (fMRI) activation between the fixing and fellow amblyopic eyes of ten strabismic amblyopes.
2. Of specific concern was whether the function of any visual area was spared in strabismic amblyopia, as recently suggested by both positron emission tomography (PET) and fMRI studies, and whether there was a close relationship between the fMRI response and known psychophysical deficits.
3. To answer these questions we measured the psychophysical deficit in each subject and used stimuli whose relationship to the psychophysical deficit was known.
4. We observed that stimuli that were well within the amblyopic passband did produce reduced fMRI activation, even in visual area V1. This suggests that V1 is anomalous in amblyopia. A similar level of reduction was observed in V2.
5. In two subjects, we found that stimuli outside the amblyopic passband produced activation in visual area V3A.
6. We did not find a close relationship between the fMRI response reduction in amblyopia and either of the known psychophysical deficits even though the fMRI response reduction in amblyopia did covary with stimulus spatial frequency.

Strabismic amblyopia in humans is composed of two different and possibly unrelated deficits: reduced contrast sensitivity (Gstalter & Green, 1971; Hess & Howell, 1977; Levi & Harwerth, 1977) and increased positional uncertainty (Levi & Klein, 1985; Hess & Holliday, 1992). The neurophysiological basis of these deficits is still unclear. Relatively subtle alterations have been found in the receptive field properties of single striate cells in cat cortex (Chino *et al.* 1983). These range from reduced contrast sensitivity of high spatial frequency cells in cat cortex (Crewther & Crewther, 1990) to reduced spatial acuity of cells in severely amblyopic monkeys (Kiorpes *et al.* 1998). These single cell abnormalities in primates appear to be mainly restricted to central vision and to be insufficient to fully account for the behavioural loss in contrast sensitivity (Kiorpes *et al.* 1998). There is a clear loss in the proportion of binocular cells in animals with strabismic amblyopia and also, at least in some severely amblyopic monkeys (Baker *et al.* 1974; Crawford & von Noorden, 1979; Fenstermaker *et al.* 1997), a loss in the proportion of cells driven by the amblyopic eye (Kiorpes *et al.* 1998). Taken as a whole, a strong case cannot be made for the above single cell deficits in visual area V1 alone forming the basis of a satisfactory explanation for the characteristic psychophysical deficits. There are two

possibilities: (1) individual cellular responses may be less affected than more global neural network responses (Schmidt *et al.* 1999), and (2) more profound single cell spatial anomalies may occur in areas beyond primate V1 (Kiorpes *et al.* 1998).

The second possibility, namely that the deficit is beyond V1, has received support from two recent brain-imaging studies, one using positron emission tomography (PET; Imamura *et al.* 1997) and the other, functional magnetic resonance imaging (fMRI; Sireteanu *et al.* 1998). Other brain-imaging (Demer *et al.* 1988; Kabasakal *et al.* 1995; Anderson *et al.* 1999) and evoked potential studies (Arden & Barnard, 1979; Levi & Nanny, 1982; Kubova *et al.* 1996) suggested that there was reduced activity in area V1 for individuals with strabismic amblyopia. Thus it is still unclear whether the earliest cortical site of human strabismic amblyopia is in V1 or the extra-striate cortex and how the cortical deficit revealed by brain imaging relates to the psychophysical loss.

To address these issues we used the tools of brain imaging that allow a measure of cortical function in humans that extends to large groups of cortical cells in different, but well-identified, striate and extra-striate visual areas. We measured cortical function using fMRI in a group of

human strabismic amblyopes. Our aims were twofold: (1) to determine whether the function of any visual area was spared in strabismic amblyopia, and (2) to assess whether the nature of any reduced cortical function could be used as a basis for explaining either of the two known psychophysical deficits.

METHODS

Subjects

Table 1 shows the clinical data for the ten amblyopic subjects used. Clinically, amblyopia in humans can be subdivided into pure strabismus without anisometropia, pure anisometropia without strabismus and a mixed form where strabismus and anisometropia coexist. From the psychophysical standpoint, this can be simplified into strabismic (with or without anisometropia) and non-strabismic (anisometropia in isolation) forms. The way the anomaly is distributed across the visual field (Hess & Pointer, 1985), its dependence on retinal illuminance (Hess *et al.* 1980) and the extent to which there is an associated spatial uncertainty (Hess & Holliday, 1992) have been shown to depend on whether there is a strabismus present, not on whether there is anisometropia. Hence a more

functional classification is in terms of strabismic and non-strabismic amblyopia. While the majority of the amblyopes used in this study do have anisometropia (the exceptions being CT, SB, MG, MS and BC), it is their strabismus that classifies them as strabismic amblyopes. During both the fMRI and psychophysics sessions, subjects wore non-magnetic spectacles to give them corrected acuity based on auto-refraction. All normal control subjects had 6/6 acuity or better in both eyes when corrected. During the scanning sessions, subjects lay on their backs and used a dental bite bar to help minimize head movement. Subjects viewed a stimulus projected at the back of the scanner bore through an angled mirror. All studies were performed with the informed consent of the subjects, conformed with the Declaration of Helsinki, and were approved by the Montreal Neurological Institute Research Ethics Committee.

Stimuli

Three basic classes of stimuli were used in this experiment: radial sinusoidal grating stimuli of variable spatial frequency (SF) and field size (Fig. 1A), structured and unstructured arrays of Gabor patterns (Fig. 1B and D), and standard retinotopic wedge and annulus checkerboard sections for retinotopic mapping. During experiments in which eyes were compared, the subject wore LCD (liquid crystal display) shutter glasses (Translucent Technologies) and viewed the screen monocularly. The LCD glasses were used to swap the subject's viewing eye before the start of each fMRI acquisition run (an experimental session typically consisted of 3 acquisition runs per eye). Stimuli were presented in a block design paradigm (see Fig. 2) whilst the subject attended to a randomly changing (from black to white) fixation spot (Fig. 1C). All stimuli were back-projected onto a translucent screen using an NEC 820 LCD video projector. Grating and Gabor stimuli were generated using a Cambridge Research Systems visual stimulus generator (VSG 2/3) card in a Gateway2000 PC. The retinotopic mapping stimuli were generated on an O2 Silicon Graphics computer.

Grating stimuli. Grating stimuli (Fig. 1A) were green–black radial sinusoidal gratings at 50% contrast forming a concentric pattern of diameter 5.4 deg and temporally sinusoidally modulated at 8 Hz. During each run, gratings of two different spatial frequencies, chosen based on the subject's acuity, were presented alternately. The lower spatial frequency presented (typically 4 c.p.d.) was well within the subject's acuity whilst the higher spatial frequency was chosen to be either above or close to the subject's amblyopic acuity limit (typically 11–22 c.p.d.). Gratings were presented for a pseudorandom interval of 21 ± 3 s and were preceded by a blank period (just fixation) of 21 ± 3 s (see Fig. 2). The fixation spot (Fig. 1A–D) subtended 0.2 deg diameter and changed randomly from black to white 25 times per acquisition run during both stimulus and blank periods. The subject was asked to press the right mouse button for fixation changes to black and the left button for changes to white. In order to check that differences in cortical response between experimental conditions were not due to attention effects, the subject's percentage correct responses were recorded.

Retinotopic stimuli. The subject viewed the stimulus monocularly with the fixing eye. We used standard retinotopic mapping techniques (Engel *et al.* 1994; Sereno *et al.* 1995) to create polar angle and eccentricity maps of the visual cortex. For polar angle and eccentricity mapping, we used rotating 90 deg wedge and expanding annuli sections of a radial checkerboard, respectively. The radial checkerboard was at 80% contrast, contained 20 radial spokes, 10 concentric bands and subtended a visual angle of 34 deg. Each stimulus rotated or expanded at a rate of 10 cycles per scanning run (1 cycle every 36 s). The checks contrast reversed at a rate of 4 Hz. The subject was instructed to attend to a central fixation triangle (radius, 0.2 deg) and to press the mouse button corresponding to the triangle direction at the end of each 3 s scan.

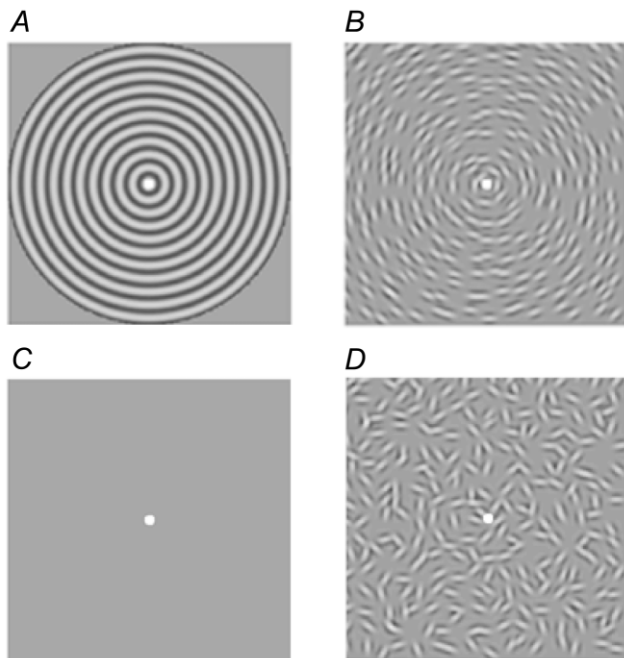


Figure 1. The generic stimulus set used in this study

All stimuli consisted of a fixation spot of radius 0.1 deg randomly changing from black to white throughout the presentation (A, B and D) and blank (C) periods. A, radial grating pattern: fixation radius, 0.1 deg; contrast, 50%; field size, 5.4 or 26 deg; spatial frequency from 4 to 20 c.p.d.; contrast reversing at 8 Hz. B, concentrically oriented Gabors: 4 c.p.d.; $\sigma = 0.1$ deg; 50% contrast; contrast reversing at 8 Hz; field size, 5.4 deg. C, blank period stimulus consisting of just a mean luminance screen and randomly changing fixation spot. D, the Gabors of stimulus B but with shuffled orientations.

Table 1. Summary of the clinical data on the amblyopes used in the study

Subject	Age/sex (years)/(M/F)	Amblyopic eye/type	Age at 1st patching/surgery (years)	Acuity	Grating acuity (c.p.d.)	Correction	Fixation	Strabismus (deg)
CT	40/F	LE/Strab	6/none	6/6 6/60	18	PL PL/+3.25 × 90	Central 3.0S	5 LET
SB	35/M	LE/Strab	None/none	6/6 3/60	11	-0.5DS +1.5DS	Central 1.0–2.0NS	2 LET
MG	18/F	RE/Strab	5/none	6/30 6/6	21	+1.75DS +1.50DS	2.0N Central	10 LXT
MS	22/F	LE/Strab	9/none	6/18 6/6	24	+0.75DS +1.0DS	Central Central	2 LET
CP	40/F	RE/ Strab–Aniso	5/none	6/18 6/6	30	-5.25/-2.25 × 180 -3.0/-1.75 × 170	2.0T Central	Intermittent 5 RXT
VE	65/M	LE/ Strab–Aniso	None/none	6/6+2 6/24	16	+1.75DS +2.5DS	Central Central	6 LXT
BC	30/M	RE/Strab	None/none	6/15–2 6/5	21	+2.0/-2.0 × 10 +2.0/-1.0 × 80	Central Central	6 RET
JF	30/M	LE/ Strab–Aniso	None/none	6/4–5 6/72	10	-2.25/-1.5 × 5 -3.00/-4.25 × 180	Central 3.0N	5 LET
OA	17/M	RE/ Strab–Aniso	Not available	6/24 6/9	13	+4.50/-5.00 × 30 -1.75/-1.75 × 150	4.0NS Central	5 RET
RD	39/M	LE/ Strab–Aniso	None	6/6 6/80	8	+0.25/-0.50 × 20 -2.5DS	1.0N	4 LET
PY	20/M	RE/ Strab–Aniso	5/patching	2/60 6/6	3.5	-8.50/-1.00 × 120 -4.00/-1.00 × 165	3.0N	10 RXT

M, male; F, female; c.p.d., cycles per degree; LE, left eye; RE, right eye; Strab, strabismic amblyopia; Aniso, anisometropic amblyopia; PL, plano; DS, dioptre sphere; N, nasal; I, inferior; S, superior; T, temporal; ET, esotropia; XT, exotropia. Entries for Acuity, Correction and Fixation columns are quoted for right and left eyes, respectively.

Acquisition

A Siemens 1.5 T Magnetom scanner was used to collect both anatomical and functional images. Anatomical images were acquired using a head coil (circularly polarized transmit and receive) and a T1-weighted sequence (repetition time (TR) = 22 ms; echo time (TE) = 10 ms; flip angle = 30 deg) giving 170 sagittal slices of 256 × 256 1 mm³ image voxels. Functional scans for each subject were collected using a surface coil (circularly polarized, receive only) positioned beneath the subject's occiput. Each functional imaging session was preceded by a surface-coil anatomical scan (identical to the head-coil anatomical sequence, except that 80 256 × 256 sagittal images of slice thickness 2 mm were acquired) in order to later coregister the data with the more homogeneous head-coil image. Functional scans were multislice T2*-weighted, gradient-echo, echo planar images (GE-EPI, TR = 3.0 s, TE = 51 ms, flip angle = 90 deg). A typical image volume consisted of 12–16 slices parallel to the calcarine sulcus. The field of view was 256 mm × 256 mm, the matrix size was 64 × 64 with a thickness of 4 mm giving voxel sizes of 4 mm × 4 mm × 4 mm. For the grating experiments, each acquisition run consisted of 115 image volumes acquired at 3 s intervals. Typically, each grating experiment consisted of six (3 fixing, 3 amblyopic eye) acquisition runs plus the surface-coil anatomical scan. The retinotopic mapping studies, acquired on a separate occasion, consisted of four acquisition runs (2 eccentricity, 2 phase) each of 128 image volumes acquired at 3 s intervals.

Pre-processing

The first three scans of each functional run were discarded due to start-up magnetization transients in the data. Also, in order to exclude voxels lying outside the head, only those functional voxels above a certain mean intensity level were included in the functional analysis procedure. As a precursor to motion correction, the functional images were corrected for image intensity variations across slices by multiplying each slice by a constant factor across all time frames. This gives a set of images where the mean slice intensity matches the mean intensity of all slices. The images were then blurred using a 3-D Gaussian window of full-width-half-maximum (FWHM) 6 mm.

Motion correction and averaging

Motion correction was performed in two stages using the AIR 3.0 package (Woods *et al.* 1998). Within each run, all functional volumes were aligned to the 64th image volume. Across runs, the run-corrected data were aligned to the mean image volume of time frames 48–80 from the first run-corrected data set. Overall head motion during both fixing and amblyopic eye stimulation was recorded. For each subject, the three normalized, smoothed, coregistered acquisition runs for each eye were used to make three average data files: average response during fixing eye stimulation, average response during amblyopic eye stimulation, and an average response of both eyes (formed from all 6 acquisition runs).

Transformation

Transformation matrices to align the surface-coil anatomical scans to the head-coil anatomical scans were calculated using an automated script combining correction for intensity gradient (Sled *et al.* 1998) and intra-subject registration (Collins *et al.* 1994; Maes *et al.* 1997). In turn, the transformation matrices of the head-coil anatomical scans into the stereotaxic space of Talairach & Tournoux (1988) were calculated (Collins *et al.* 1994; Maes *et al.* 1997). Using these transforms, an occipital lobe template, defined in Talairach space, was created for each functional data set. Typically the identified occipital region contained around ~ 3000 1 mm^3 functional brain voxels and $\sim 10\,000$ non-occipital voxels.

Correlation

Predicted haemodynamic response curves (or stimulus vectors) for each stimulus were formed by convolving a linear systems approximation of the haemodynamic response function (Boynton *et al.* 1996; delay time = 4 s, time constant = 1.6 s) with the stimulus

on-off time sequence. Generally, we found rank order, rather than linear, correlation to be a more robust identifier of fMRI activation, presumably as it is less sensitive to spurious spikes in the data (Press *et al.* 1992). In order to observe the effect of interleaved stimuli using a rank order technique it was necessary to splice the data from each time series into two overlapping sets. Each set contained all the data except those where the predicted haemodynamic response of the alternative stimulus exceeded 5% of its maximum value. In this way it was possible to produce individual *t*-maps for high and low spatial frequency stimuli. After this subdivision, each time series contained 67 data points. For voxels in the occipital lobe, assuming a resolution element size of $6 \text{ mm} \times 6 \text{ mm} \times 6 \text{ mm}$ (after smoothing), 65 degrees of freedom, and correcting for multiple comparisons, a *t* value of 4.12 was found to correspond to a significance level of $P < 0.05$.

Measures of the BOLD response

In order to condense the considerable amount of data obtained for each subject we chose two measures of cortical activation. Firstly, in

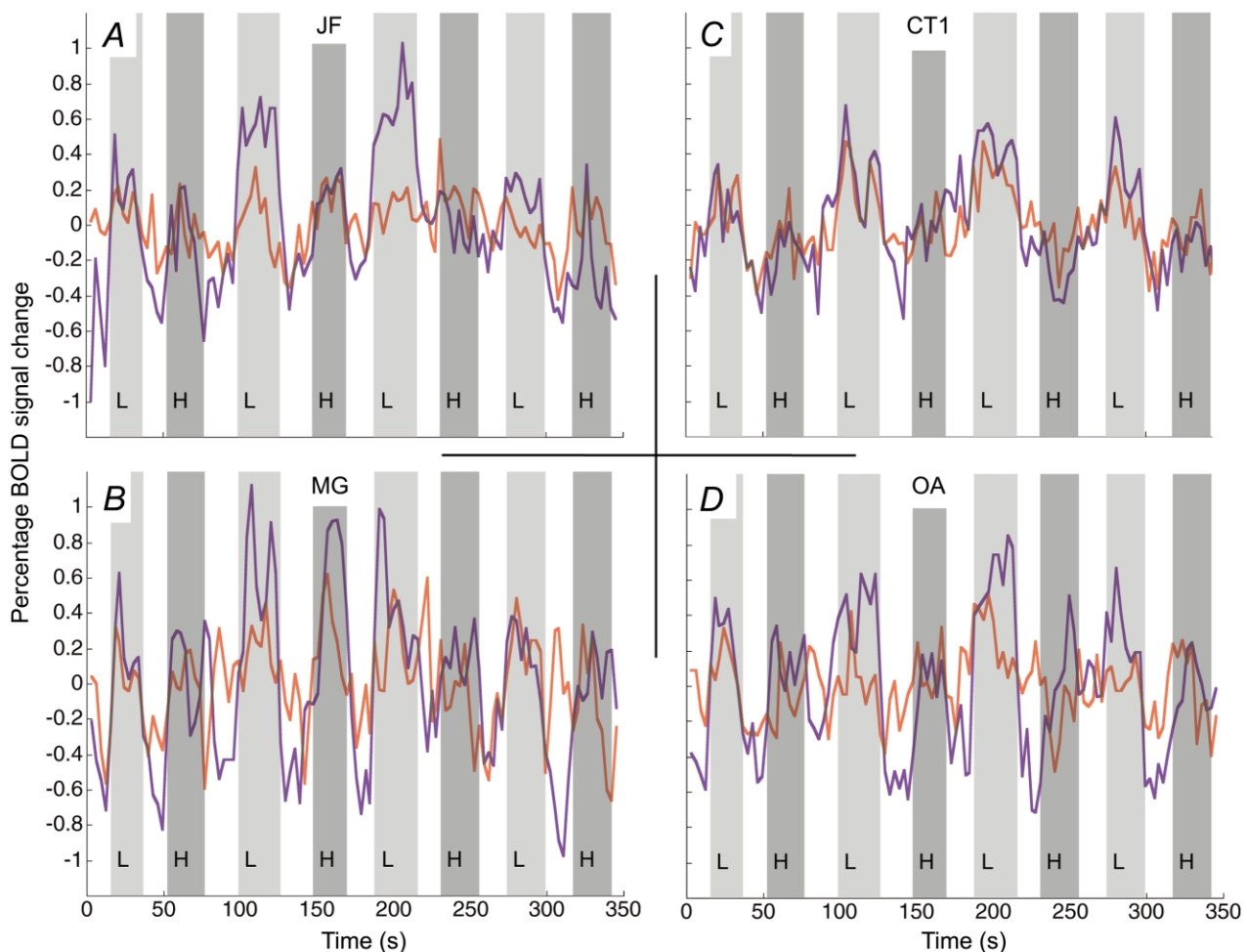


Figure 2. Time course of BOLD signal change for amblyopic (red) and fixing eye (purple) stimulation for four subjects

The light and dark grey bars indicate the presentation of low (L) and high (H) spatial frequency stimuli, respectively; the bars have been delayed in time by 6 s in order to coincide with the time-lagged haemodynamic response. The open bars show the blank stimulus condition where no grating stimuli were presented. Time series were created using the voxels identified as significantly active from the average response of both eyes to the low spatial frequency stimulus. Note that in all subjects except CT the response for amblyopic, as compared to fixing eye, stimulation was reduced.

order to quantify the intensity of activation, we measured the percentage BOLD (blood oxygenation level dependence) change per voxel within a specified template. Secondly, in order to quantify the spatial extent of activation, we measured the number of voxels reaching a criterion significance level ($P < 0.05$).

BOLD percentage change. In order to quantify the intensity of neuronal activation it was necessary to select a specific voxel subset or template. The average time series of the percentage voxel intensity change across this subset was calculated. Gram-Schmidt orthogonalization was then used to calculate the optimal weights projecting each of the stimulus vectors onto the average (Bandettini *et al.* 1993). Error bars for this estimate were given from the standard deviation of the data unaccounted for after subtraction of the projections of both stimulus vectors. The template was defined as those voxels that were significantly ($P < 0.05$) correlated with the low spatial frequency stimulus in the both-eyes average data file. That is, those areas of cortex that were measured as responsive to visible visual stimuli presented to either or both eyes. This method has the advantage that it is based on a pooled BOLD response and so may be more sensitive to small changes in cortical oxygenation level; however, the amplitude of the response will depend on the subset of voxels chosen for the template.

Number of voxels. As a measure of the extent of activation we used the number of voxels in the t -statistic images that reached a significance level of $P < 0.05$. Although voxel counting is known to be unstable (Cohen & DuBois, 1999), we found that this measure well summarized the level of stimulus-correlated activation in the t -statistic maps (compare Figs 3A and 5 for subjects JF, MG, OA and CT). As stimulus-correlated head movement and purely random factors such as scanner noise spikes can artificially raise the threshold that distinguishes stimulus-related neuronal activity from artefact, error bars were plotted that indicate the relative proportion of the voxels outside the occipital lobe that also reached this significance level. Clearly, this method is insensitive to changes in the BOLD signal that do not cross the preset threshold, but it has the advantage that it is not biased towards any particular voxel subset.

Cortical flattening

We used the Stanford-developed software mrGray and mrUnfold tools (Engel *et al.* 1997; Teo *et al.* 1997) to semi-automatically classify grey and white matter within the occipital lobe and then to unfold it, with minimal distortion, into a flat sheet. Typically, an area of 6 cm radius was unfolded from around a point within the calcarine fundus and 3 cm anterior to the occipital pole. The software returns coordinate arrays that map points in the flattened representation to the anatomical volume. For each retinotopic data set, magnitude and phase images of the fundamental Fourier component were created. These images were then transformed and resampled to the same space as the classified grey/white matter volume. Using the point–point correspondence derived from the flattening, each point in the phase image with a magnitude value above a certain threshold was plotted onto the flat map. Horizontal and vertical meridians were identified from the maxima and minima in plots of the absolute cosine of the mapped polar angle. Non-retinotopic functional data were transformed to the flat map in a similar manner, with the exception that the files were presmoothed with a 3-D Gaussian kernel (FWHM = 12 mm) after resampling.

Psychophysics

Eye occlusion. To test monocular function we occluded either the fixing or fellow amblyopic eye with LCD shutters. This was done for both the psychophysical testing and for the brain imaging. In the occluded state, the LCD lens was totally diffuse. Under these conditions there is no binocularly mediated suppression of the

amblyopic eye since all pattern vision in the good eye has been abolished (Harrad & Hess, 1992).

Grating acuity. For each subject, grating acuity for the corrected amblyopic eye was established using a method of constant stimuli and a two alternative forced choice (2AFC) protocol. The two intervals were the flickering grating with fixation spot and just fixation spot. The subject's percentage correct identification of the interval containing the grating was measured over fixed spatial frequency steps from 2 to 22 c.p.d. For the fMRI experiment, gratings were generated using the VSG 2/3 card and projected using the NEC 820 LCD video projector. Grating contrast was set at 50%.

Contrast sensitivity. Contrast sensitivity measures were made using a VSG 2/3 card and NEC Multisync XP 17 monitor. Contrast sensitivity to each of the grating stimuli was measured using a 2AFC protocol and a PEST algorithm. Data were fitted with a Weibull function to determine contrast sensitivity thresholds for each of the stimuli used. Sensitivity is plotted as decibels (dB) of attenuation from 100% Michelson contrast, i.e. Sensitivity = $20 \log_{10}(100/(\% \text{ contrast}))$.

Contrast matching. For two subjects contrast matches between fixing and amblyopic eye were also measured. The LCD shutter glasses were used to alternately, at a rate of 1 Hz, occlude one eye whilst the other eye viewed the 4 c.p.d. stimulus at a certain contrast level. The contrast of the grating presented to the amblyopic eye was held constant at 50% and the subjects were asked to adjust the contrast of the grating presented to the fellow eye until it appeared at equal contrast. Eight matches were made from different initial contrasts. Gratings were generated using the VSG 2/3 card and projected using the NEC 820 LCD video projector.

Optical correction

All subjects underwent objective refractions to determine what correction optimized the contrast of the retinal image. This included auto-refraction (Canon R-22) as well as retinoscopy. We considered a subjective refraction inadequate for this project because in severe cases its accuracy is compromised by the depth of amblyopia. Since we wanted to assess the performance of V1, if the site of the amblyopic disturbance is upstream from V1, then our assessment would have been invalidated if the clarity of the retinal image was not optimal.

RESULTS

Stimuli invisible to the amblyopic visual system

In order to test whether the occipital cortex and in particular the striate cortex was normal in strabismic amblyopia (Imamura *et al.* 1997; Sireteanu *et al.* 1998), we set out to determine whether normal fMRI responses could be obtained to stimuli that were essentially invisible to the amblyopic visual system as a whole. This would be expected if the striate cortex was normal and the cortical deficit in amblyopia was located exclusively in the extra-striate cortex. Because of the limited spatial resolution of the LCD projector, only some of our amblyopic subjects could be used, namely those with the most severe amblyopia (CT, JF, SB, VE, PY, RD; see Table 1). Using the method of constant stimuli we measured the psychophysical acuity (see Table 1) of each amblyope for the actual spatio-temporal pattern (i.e. Fig. 1A, contrast reversing at 8 Hz) to be used in the subsequent brain imaging.

In Fig. 3*B* and *D*, two indices of cortical activation are plotted: the number of voxels reaching the $P < 0.05$ significance criteria and the average percentage BOLD change observed within a predefined voxel template. Respectively, these are measures of the amount of cortex activated and the intensity of this activation (see

Methods). The abscissa is the ratio of the stimulus spatial frequency to the 50% point on the acuity psychometric function (2AFC) for the amblyopic eye. A value of 1 represents a stimulus whose spatial frequency was undetectable by the amblyopic eye (i.e. at chance levels of performance). The activation when viewing through the

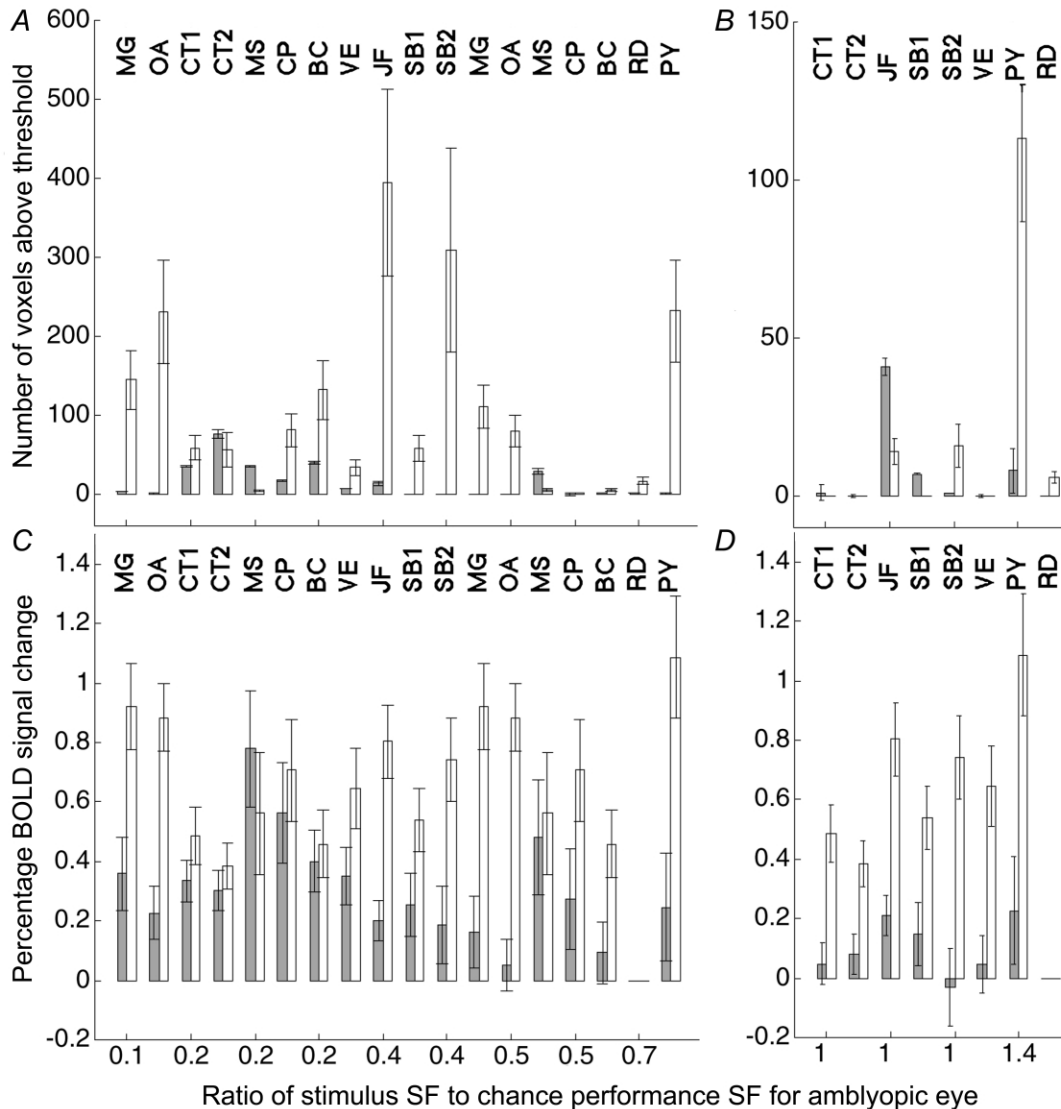


Figure 3. Summary of the overall activity level in the occipital cortex during amblyopic (grey bars) and fixing (open bars) eye stimulation for the ten subjects used in the study

The abscissa denotes the ratio of the stimulus spatial frequency to the spatial frequency at which the subject is at chance performance using the amblyopic eye: in *A* and *C* the stimuli were within the acuity range of the amblyopic eye, whereas in *B* and *D* the stimuli were not detectable using this eye. Two measures are presented: total number of voxels reaching significance (*A* and *B*) and mean percentage BOLD signal change (*C* and *D*). For *C* and *D*, the percentage change data are based on those voxels identified as significantly active from the average response of both eyes to the low spatial frequency stimulus. *A*, in all subjects except CT and MS, there was a considerable reduction in the number of voxels that reached significance when the amblyopic eye was stimulated. *B*, only subject JF (and possibly SB1) showed activation when the amblyopic eye was stimulated with a grating that was beyond the subject's acuity. Note that for CP, CT and VE, even during normal eye viewing of the high SF stimulus, no voxels reached the significance criterion. *C*, the general decrease in activity level during amblyopic eye stimulation observed in *A* was also seen when percentage BOLD signal change was measured. *D*, as in *B*, only subject JF showed a definitive response to a grating that was beyond his amblyopic eye's acuity.

normal eye is indicated by open bars and that through the amblyopic eye by grey bars.

The figure helps to illustrate the relative merits of the two measures used. For example, in some subjects (see CT and VE; Fig. 3*B*), even during normal eye stimulation, no individual voxels reached the preset significance level ($P < 0.05$). That is not to say that there was no cortical activation during these conditions, but rather that there was no individual image voxel where there was a stimulus-correlated change in blood oxygenation level of sufficient magnitude to cross the 5% significance threshold. However, as the responses from individual voxels were averaged together, percentage BOLD signal changes became visible above the noise (Fig. 3*D*). In other words, the sample size used to create Fig. 3*D* was larger for that used in Fig. 3*B*; the average measurement therefore has smaller standard error and small changes in cortical blood oxygenation become observable above the noise. That said, identifying the voxel subset or template for Fig. 3*D* has the complication that these voxels must equally sample the cortical regions stimulated by each eye whereas the voxel measures in Fig. 3*B* have no such potential for bias. As stated in Methods, the template was defined as those voxels that were significantly ($P < 0.05$) correlated with the low spatial frequency stimulus in the both-eyes average data file. This voxel subset was chosen as it was an unbiased average from both eyes to a suprathreshold stimulus. It is possible that, despite the small field size (5.4 deg diameter), different voxels are optimally activated by the high and low spatial frequency stimuli. It should be noted that we were not comparing changes in response as spatial frequency was varied, but rather changes in the balance of activation between eyes. That is, in the extreme case where voxels activated by the high spatial frequency stimuli did not overlap with those in the template, one would expect, due to our analysis method, a reduction (to zero) in the percentage BOLD response measure, but this reduction would be the same for both amblyopic and normal eye viewing. The choice of a low SF template therefore could account for an amplitude difference in the percentage BOLD change between high and low SF responses but not differences observed between eyes.

Only two subjects (JF and SB1) showed significant activation for both indices of brain activation when the amblyopic eye was stimulated with stimuli beyond the psychophysical acuity limit. Of these, only JF exhibited a consistent (see SB2 which is a repeat of SB1) and large response when the amblyopic eye was stimulated. The anatomical site of this activation is shown in Fig. 4*A* for the high spatial frequency stimulus (11 c.p.d.) where the activation for both the fixing (green voxels) and fellow amblyopic (red voxels) eye stimulation is superimposed on the anatomical scan. The activity was located on the dorso-lateral surface of the occipital lobe (Talairach coordinates, left hemisphere: $x = -34 \pm 3$, $y = -89 \pm 4$, $z = 5 \pm 5$; right hemisphere: $x = 25 \pm 5$, $y = -91 \pm 4$,

$z = -6.5 \pm 5$). This was similar for SB1 (Talairach coordinates, right hemisphere: $x = 32 \pm 4$, $y = -85 \pm 5$, $z = 10 \pm 10$). Figure 6 shows this activation overlaid as a blue contour on a flattened representation of JF's right occipital cortex alongside cortical area boundaries from the retinotopic mapping study. From our retinotopic map, the activation appeared to lie at the dorsal V3–V3A boundary. The disparity between the site of activation (due to a 2.7 deg radius stimulus) and the confluent foveal representation of areas V1–V3 suggested that the focus of activity was within area V3A, which has its own foveal representation (Tootell *et al.* 1997), and not V3. Also, other studies (Tootell *et al.* 1997; Smith *et al.* 1998) have identified the foveal section of V3A and their coordinates ($x = \pm 39$, $y = -86$, $z = -16$; $x = \pm 26$, $y = -89$, $z = -2$, respectively) correspond well with the regions of activation observed in both SB1 and JF.

Stimuli visible to the amblyopic visual system

Amblyopia is characterized not only by a restricted passband but also by reduced contrast sensitivity for stimuli that fall within this passband. While this contrast sensitivity deficit can affect low as well as high spatial frequencies (Hess & Howell, 1977), it is usually greater at high spatial frequencies (Gstalder & Green, 1971; Hess & Howell, 1977; Levi & Harwerth, 1977). We chose to use a spatial frequency target within the passband of all our subjects to assess cortical function using fMRI. The stimulus was the same as before (see Fig. 1*A* and Methods) and its contrast was 50%. From our psychophysical measurements of acuity we were able to estimate how close the stimulus spatial frequency was to the acuity of the amblyopic visual system, and this was indicated as a ratio as previously described. The results are shown in Fig. 3, where the brain activation in the occipital cortex is plotted in terms of our two indices: the number of voxels reaching significance (Fig. 3*A*) and the percentage BOLD signal change (Fig. 3*C*). The activation due to stimulation through the normal eye is indicated by open bars and that through the amblyopic eye by grey bars. In general, the measured cortical activation decreased when the amblyopic eye was stimulated although this decrease did not seem to relate to the subjects' acuity deficit. This can be seen in the averaged time series (Fig. 2*A*, *B* and *D*, light grey bars represent responses for the low spatial frequency) for subjects JF, MG and OA. There were, however, some notable exceptions; subject CT (i.e. CT1, CT2) showed similar levels of activation (see Fig. 3*A* and *C* as well as the time series, Fig. 2*C*) for both eyes and subject MS showed a larger extent of activation (in terms of voxels reaching significance) when stimulation was through the amblyopic eye. Note that in general the response to the high SF stimulus was less than that to the low SF stimulus (Fig. 3*A* and *B*). This meant that for a number of subjects (CT, VE, CT, BC and RD), even during normal eye viewing of the high SF stimulus, no voxels reached the preset significance criterion.

The extent of the difference in cortical activity when the amblyopic eye was stimulated for this lower spatial frequency target is illustrated in the statistical maps from a slice taken through the calcarine sulcus of four of the subjects (Fig. 5). Subjects JF, OA and MG showed a marked decrease in measured activation when the amblyopic eye was stimulated, subject CT1 showed similar or possibly larger activation when the amblyopic eye was stimulated. For subject JF, the regions of activation (red, amblyopic; green, fixing; purple, both) are superimposed onto the structural images in Fig. 4*B* for the low spatial frequency stimulus (4 c.p.d.). Two things are noteworthy. Firstly, the responses to high and low spatial frequency stimuli were in approximately the same cortical region (compare Fig. 4*A* and *B*). Secondly, the number of voxels reaching significance was markedly reduced for low spatial frequency stimulation of the amblyopic eye.

In order to reliably identify the contribution of the different visual cortical areas to the activation described above, we used the same lower spatial frequency stimulus

to that described above but subtending 26 deg in diameter. We used the mapping approach described by Sereno and colleagues (Sereno *et al.* 1995) to identify the visual cortical areas in a flattened representation (see Methods). The unfolded occipital lobes of four amblyopic subjects (MG, OA, JF and CP) are displayed in Fig. 6*A*. Each surface is plotted as a *t*-statistic map of activation due to fixing (right panel) and amblyopic (left panel) eye stimulation. The cortical loci corresponding to the horizontal meridia (black dashed), vertical meridia (black continuous) and iso-eccentricity lines (pink dashed) derived from the retinotopic mapping study are marked. Note that in all subjects there was a global decrease in activity across all identified visual areas (including V1) when the amblyopic (left panel) rather than the fixing (right panel) eye was stimulated. This difference in activation is quantified in Fig. 6*B*, where the mean *t* values for V1 and, in three subjects, V2 are plotted. We found a similar level of reduction for both V1 and V2. It should be noted that there were signal-to-noise limitations to our imaging technique and although the absolute level of activity was clearly reduced during amblyopic eye viewing, the

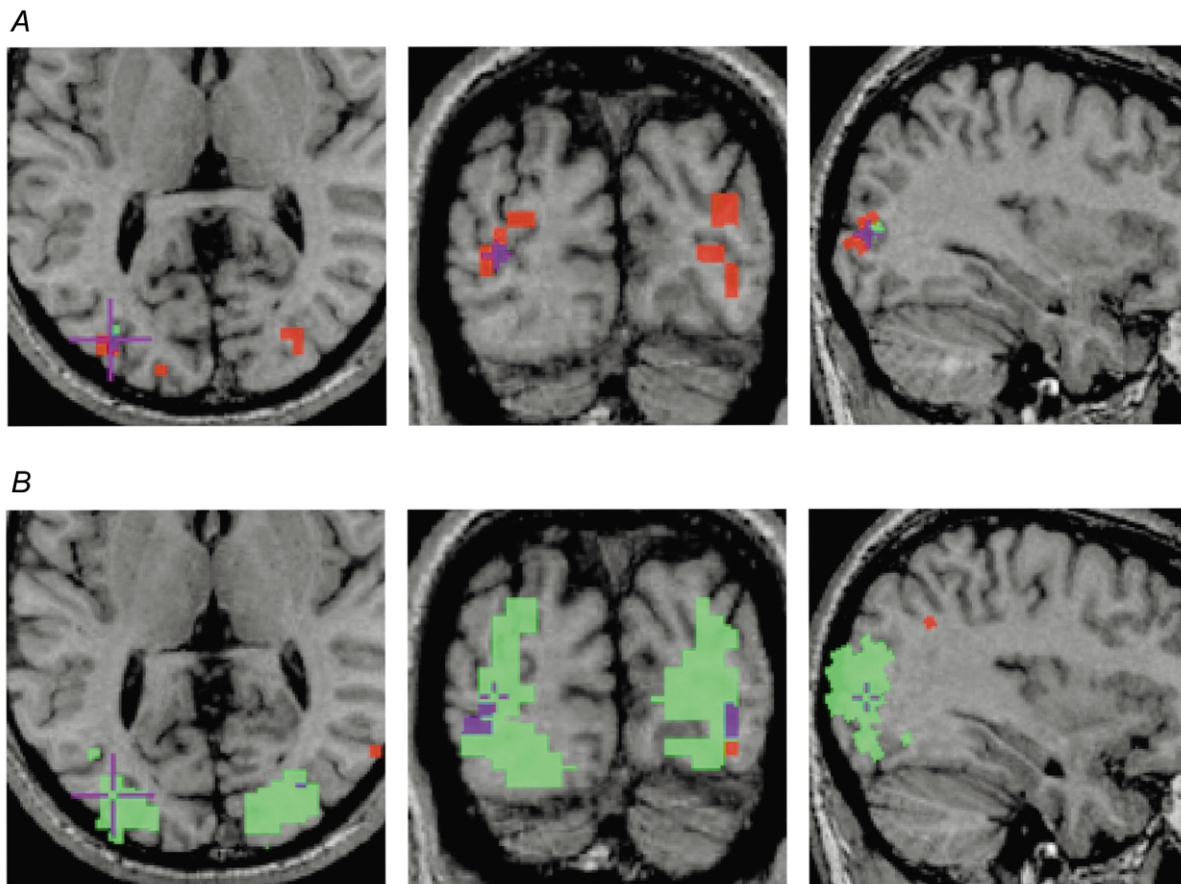


Figure 4. Axial (left), coronal (middle) and sagittal (right) anatomical images of subject JF

Significant ($P < 0.05$) functional voxels during fixing (green) and amblyopic (red) eye stimulation are superimposed. Purple is used to show the area of overlap. *A*, response to the 11 c.p.d. grating. Note that this grating was beyond JF's amblyopic eye acuity, yet there was significant activation when this eye was stimulated. *B*, the response to the 4 c.p.d. grating shows a large area of cortex driven by the fixing eye, yet relatively little detectable activation when the amblyopic eye was stimulated.

absence of a measured BOLD response does not necessarily mean that these cortical areas were not active.

Relationship between the psychophysical and brain imaging deficits. It is tempting to ascribe the brain imaging deficits observed in the majority of the strabismic amblyopes studied here to their reduced contrast sensitivity. However, the relationship may not be straightforward. The stimulus that we used had a spatial frequency of 4 c.p.d. and a contrast of 50%. In Fig. 7, the relationship between the more robust measure of brain activation, namely the normalized difference in percentage BOLD signal change between the two eyes (see eqn (1)) and various psychophysical measures (absolute and relative contrast sensitivity and acuity), are plotted.

$$\text{Normalized difference} = \frac{B_{\text{Fix}} - B_{\text{Amb}}}{B_{\text{Fix}} + B_{\text{Amb}}}, \quad (1)$$

where B_{Fix} and B_{Amb} are the mean percentage BOLD signal change (as plotted in Fig. 3C and D) during fixing and

amblyopic eye stimulation, respectively. For subjects (VE, PY, CT and SB) who could resolve the higher spatial frequency stimulus, results are displayed for both high and low spatial frequency stimulation. The results did not indicate a clear relationship (correlation (r) ~ 0.4) between any of these measures for the group as a whole. However, for some measures, individual subjects did show a consistent bias in activation towards the normal eye for the high as compared to the low spatial frequency stimulus (joined by continuous lines). This was the case when the measure was the absolute contrast sensitivity of the amblyopic eye (Fig. 7A), the absolute contrast sensitivity of the good eye (Fig. 7B) or the ratio of the stimulus spatial frequency to the amblyopic acuity (Fig. 7D). It was not the case when the measure was the contrast sensitivity difference (in dB) between the normal and fixing eyes (Fig. 7C). This was at first surprising as this has been assumed in previous imaging studies in amblyopia (Demer *et al.* 1988; Kabasakal *et al.* 1995; Imamura *et al.* 1997; Sireteanu *et al.* 1998; Anderson *et al.*

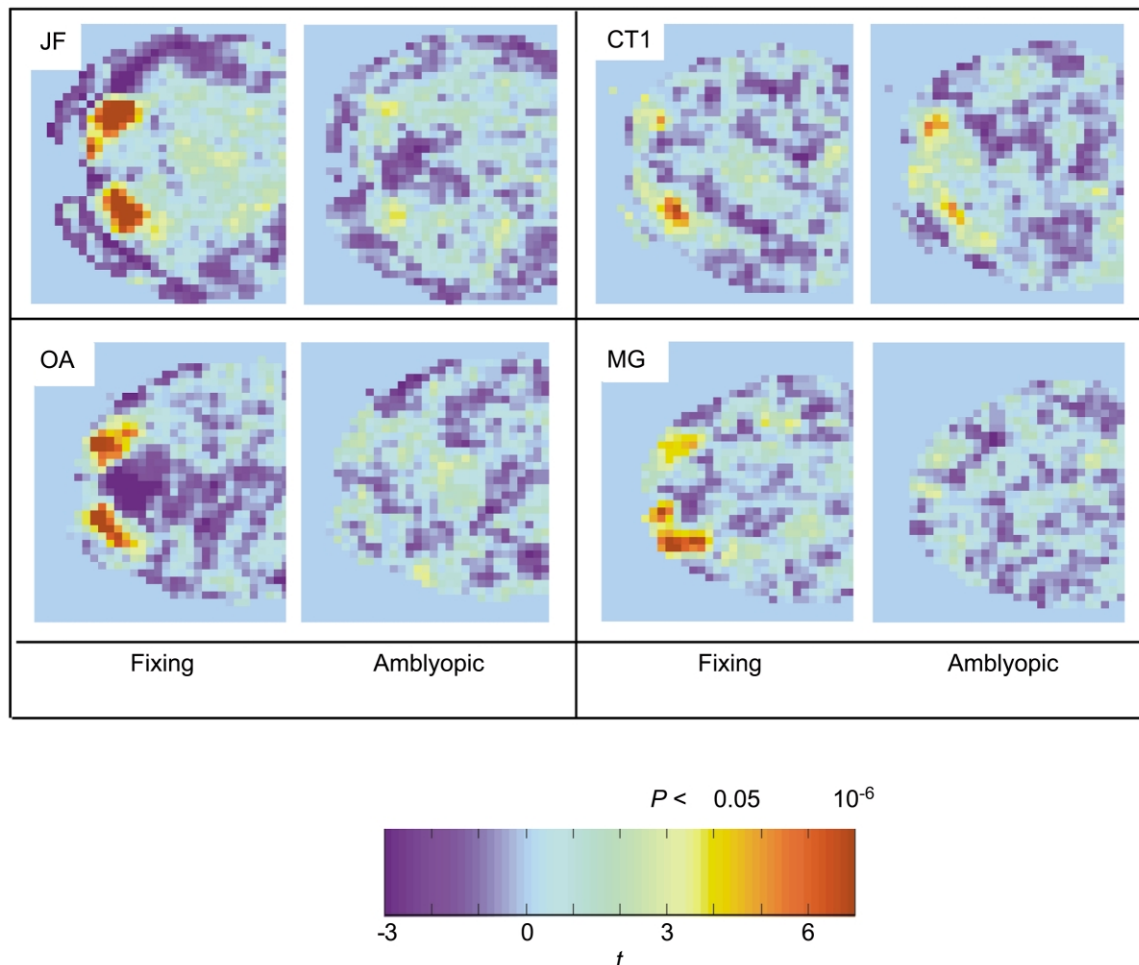


Figure 5. Colour map t -statistic images for four subjects for fixing and amblyopic eye stimulation. Each panel shows the posterior portion of a single functional slice along the calcarine sulcus; typically the activity was located at the occipital pole consistent with the cortical representation of the fovea. Note that in all subjects, except CT1, there was a marked reduction in activity for amblyopic as compared to fixing eye stimulation.

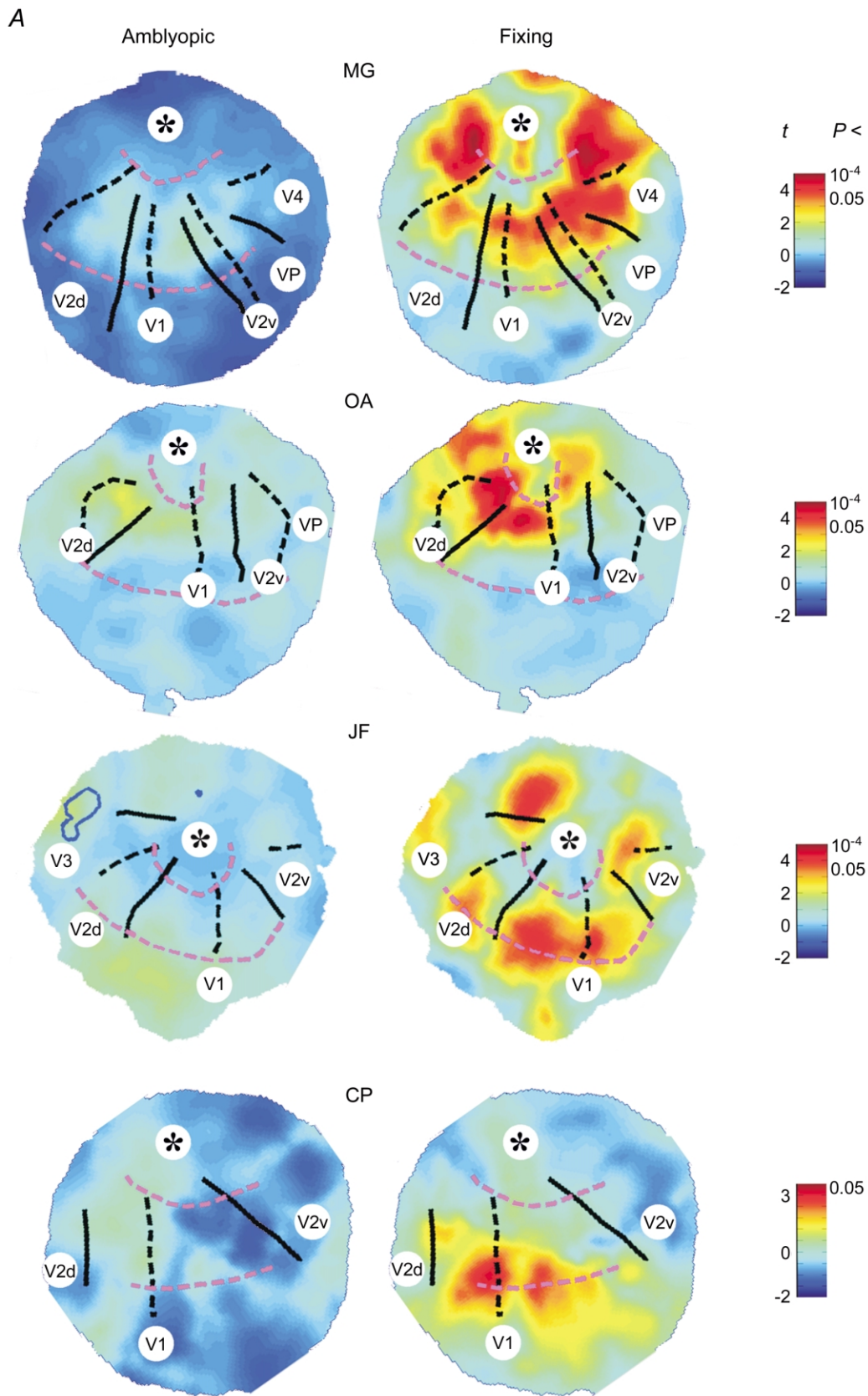


Figure 6. For legend see facing page.

1999). However, the contrast used in imaging studies is usually high (e.g. 50% in the present investigation) and contrast sensitivity is a purely threshold measure. The psychophysical correlations depicted in Fig. 7 show that it was with spatial frequency not contrast sensitivity that the brain imaging deficit covaried.

The other hallmark of strabismic amblyopia from the psychophysical perspective involves positional uncertainty (Levi & Klein, 1983; Hess & Holliday, 1992) and spatially

distorted perceptions (Hess *et al.* 1978; Bedell & Flom, 1981, 1983; Lagreze & Sireteanu, 1991; Sireteanu *et al.* 1993), which have been postulated to have a common basis, one that is different from that of the contrast sensitivity anomaly (Hess & Holliday, 1992). Strabismic amblyopes may have been able to veridically match the contrast of the stimulus used here but they did not see the two stimuli as identical. They reported spatial distortions that varied with spatial frequency and affected mainly the central field (Hess *et al.* 1978). Could it be that a

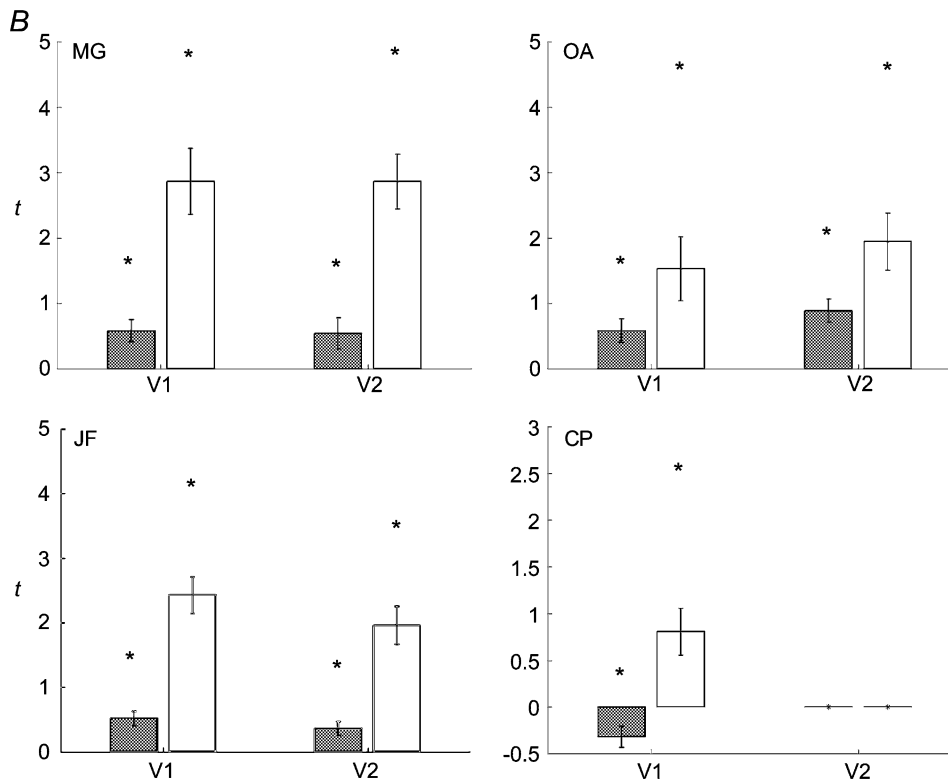


Figure 6. Activation across visual cortical areas

A, flattened occipital grey matter surfaces for subjects MG, OA, JF and CP overlaid with functional data from fixing (right panel) and amblyopic (left panel) eye viewing of the large field stimulus. The top of each map corresponds to the occipital pole, the centre is a point within the calcarine fundus approximately 3–4 cm anterior to the pole, the dorsal–ventral direction is left to right. The right occipital lobe is shown for all subjects except CP. The cortical loci corresponding to the horizontal meridia (black dashed), vertical meridia (black continuous) and iso-eccentricity lines (pink dashed) derived from the retinotopic mapping study are overlaid. The identifiable visual areas have been labelled. In all subjects V1 is clear, spanning the central region of each surface between the upper and lower vertical meridia (continuous lines) that mark its borders with ventral and dorsal V2 (V2v and V2d). Moving down from the approximate location of the cortical foveal representation in V1–V3 (*) the iso-eccentricity lines (pink dashed) are at 4 and 14 deg in turn. Functional data are overlaid on each surface in the form of a colour map, red and blue showing stimulus-correlated and -uncorrelated regions of activation, respectively. Note the change of colour map scale for subject CP who showed generally poorer activation. Note that in all subjects there was a global decrease in activity across all identified visual areas (including V1) when the amblyopic (left panel) rather than the fixing (right panel) eye was stimulated. In the case of subject JF, the locus of significant cortical activation during amblyopic eye stimulation from the subthreshold, small field, stimulus (see Fig. 4A) is outlined in blue on the flat map. This region is located at the V3–V3A border. *B*, mean *t* values (\pm S.E.M.) in visual areas V1 and V2 taken from the flat maps in *A* due to amblyopic (grey bars) and fixing eye (open bars) stimulation. Also shown (*) are the maximum *t* values within each region. Both mean and maximum *t* values show a significant decrease in activation during amblyopic eye stimulation. This decrease appeared to be equally marked in both V1 and V2.

disruption to the cortical spatial representation of the structured stimulus used here (see Fig. 1A) could in itself result in reduced brain activation? To test this we compared responses to two stimuli made up of an identical array of oriented Gabors elements; in one the element orientations were consistent with a global radial bull's-eye contour (Fig. 1B) whereas in the other the local orientations were randomized with respect to position and no global contour was visible (Fig. 1D). This manipulation

keeps the local density and global orientation statistics of the stimuli constant. In three normal observers, we assessed whether such a disruption would reduce cortical activation as assessed by fMRI. We found no large difference in brain activation in V1 of normal observers that was comparable to the change observed in amblyopia when the global structure of the stimulus we used was disrupted. While this was in no way meant to model the possible spatial distortion in amblyopia, it does suggest

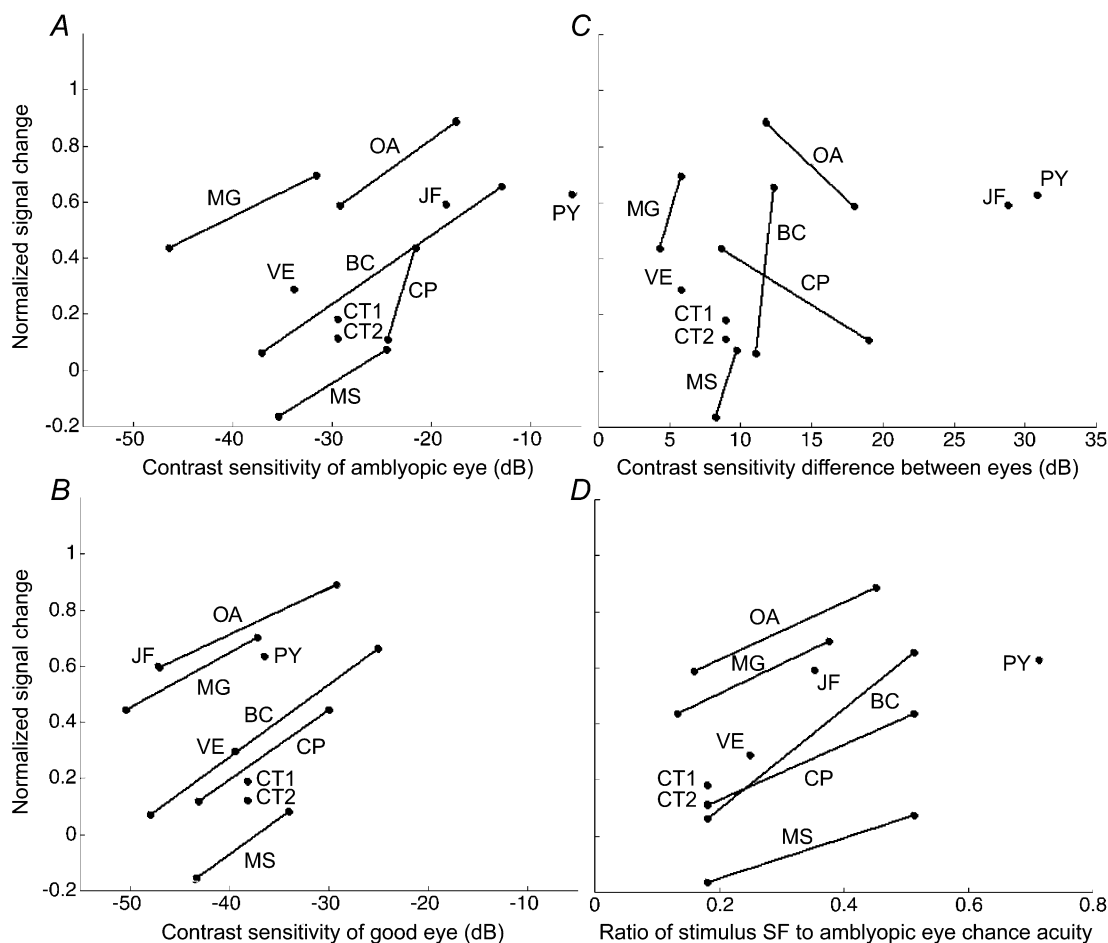


Figure 7. Scatter plots showing the data from Fig. 3C and D replotted as normalized signal difference (see eqn (1)) between BOLD signal changes for fixing and amblyopic eye stimulation

At the ordinates 1 and -1 all measured signal change is due to the fixing eye and amblyopic eye, respectively; at zero, stimulation of each eye elicits the same level of cortical activity. For only one subject (MS) and one spatial frequency, the balance of activity favoured the amblyopic eye; typically, however, data points were at positive ordinates indicating that the fixing eye tends to dominate. In the cases where both stimuli were visible when viewed with the amblyopic eye a line joins the two data points. *A*, normalized signal difference plotted against the contrast sensitivity of the amblyopic eye to the stimulus. Note from the gradient of the lines that there was a consistent trend – the poorer the contrast sensitivity (hence the higher the spatial frequency of the stimulus), the more the activity favoured the fixing eye. *B*, normalized signal difference plotted against the contrast sensitivity of the fixing eye. The same trend as in *A* is clear. *C*, normalized signal difference plotted against the contrast sensitivity difference between eyes. Interestingly, the difference in the balance of activation between eyes did not correlate with the difference in contrast sensitivity between eyes to that stimulus. *D*, normalized signal difference plotted against the ratio of stimulus spatial frequency to the spatial frequency at which the subject is at chance performance when viewing with the amblyopic eye. Again, the closer the stimulus spatial frequency to the amblyopic eye acuity limit, the more the balance of activity favoured the fixing eye.

that the highly structured nature of the stimulus used in this study was not a crucial part of the finding of an anomaly in brain activation in amblyopic subjects.

Finally, we found no systematic difference in the performance for identification of the fixation target's polarity between fixing and amblyopic eye stimulation. The fixation spot's polarity continually changed throughout the fMRI acquisitions, suggesting that the subjects were attending to the central part of the stimulus and that attentional changes *per se* cannot explain the reduced fMRI activation when the amblyopic eye was stimulated.

DISCUSSION

In the majority of strabismic amblyopes tested we could find no evidence of normal function in any visual area, including V1. This was equally true for the strabismic with and without anisometropia. Also, this was true regardless of the spatial frequency or field size of the stimulus. Stimuli whose spatial frequency was well within the amblyopic passband produced reduced brain activation for the amblyopic visual system, in line with some previous reports (Demer *et al.* 1988; Kabasakal *et al.* 1995; Anderson *et al.* 1999), though this was not confined to the extra-striate cortex as a number of previous reports have suggested (Imamura *et al.* 1997; Sireteanu *et al.* 1998). Indeed, we found the level of this reduction to be similar in V1 and V2 (Fig. 6*B*). Two subjects did display activation to stimuli outside the visibility range of the amblyopic system. For JF, our mapping data indicate that this response was localized to the V3–V3A border (Fig. 6). However, as one would expect a stimulus of 2.7 deg radius to excite the confluent foveal representations of V1–V3 (and not eccentric V3), we believe that the site of activation is within the separate foveal representation of V3A (Tootell *et al.* 1997). The Talairach coordinates of this active region also correspond closely to those from the published literature on V3A (Tootell *et al.* 1997; Smith *et al.* 1998). The explanation for this activation in JF and SB1 to stimuli outside their psychophysical visibility is puzzling. It may relate to the finding that, although the mean acuity of cortical neurons driven by the amblyopic eye is reduced in cats and monkeys with artificially induced esotropia, some isolated neurons can be found with normal acuity (Crewther & Crewther, 1990) or at least acuity above the behavioural limit (Roelfsema *et al.* 1994; Kiorpes *et al.* 1998). Given the preference of area V3A for moving stimuli (Tootell *et al.* 1997), the 8 Hz contrast reversing bull's-eye pattern would presumably be an optimal stimulus.

The reduced activation for stimuli inside the amblyopic passband was a characteristic feature of the small and large field stimulation used here. This reduced activation was in V1 as well as other extra-striate areas. In our clinical group, the contrast sensitivity differences did not correlate with the measured differences in brain

activation between fixing and fellow amblyopic eyes. Furthermore, larger field stimulation, which is known to result in smaller difference of contrast sensitivity between the eyes of strabismic amblyopes (Hess *et al.* 1980; Hess & Pointer, 1985), did not result in similar patterns of neural activation (between eyes) in four of our subjects (MG, OA, JF and CP). This lack of correlation between the contrast sensitivity and brain activation deficits is not completely unexpected because the stimulus we used was 50% contrast and as such should have been seen veridically by the amblyopic visual system (Hess & Bradley, 1980), a fact that we subsequently verified in two of our subjects (MG and OA) using an interocular matching protocol (see Methods). Subject MG's interocular contrast match was 62.8% (S.D., $\pm 4.39\%$) whereas subject OA's match was 39.7% (S.D., $\pm 12.6\%$). Neither result was significantly reduced from normal (i.e. 50%). Anderson *et al.* (1999) reported a similar lack of correlation with contrast sensitivity for the magnetoencephalographic (MEG)-evoked response in amblyopia. If the contrast sensitivity deficit is due to reduced sensitivity of neurons with low contrast thresholds tuned to higher spatial frequencies, it may not be surprising that it is not reflected in the population response on which fMRI depends. Such a neuronal deficit might be better revealed using low contrast stimuli. On the other hand, if the contrast sensitivity loss is due to fewer cells being driven by the amblyopic eye (Levi & Klein, 1985) then one would have expected a correlation between the brain imaging deficit and the contrast sensitivity loss in amblyopia.

In a number of our amblyopic subjects we were able to obtain reliable levels of activation for both the low and high spatial frequency stimuli which were interleaved in the same fMRI session. Although there was no strong group correlation between the relative activation of normal and amblyopic cortex and the various psychophysical measures used (Fig. 7), it is clear that for individual subjects higher spatial frequency stimuli produced larger differences between normal and amblyopic brain activation. This was due to spatial frequency *per se* rather than an indirect consequence of the contrast sensitivity deficit (Fig. 7*C*). Spatial frequency is the only common factor that could account for the observed correlation with the other three psychophysical measures (Fig. 7*A*, *B* and *D*). This suggests that the difference in brain activation between normal and fellow amblyopic stimulation is due to some factor, which covaries with spatial frequency, other than contrast sensitivity.

Strabismic amblyopia is characterized by positional uncertainty (Levi & Klein, 1983; Hess & Holliday, 1992; Demanins & Hess, 1996) and distorted spatial perceptions (Hess *et al.* 1978; Bedell & Flom, 1981, 1983; Lagreze & Sireteanu, 1991; Sireteanu *et al.* 1993). These are not a consequence of the contrast sensitivity loss (Hess & Holliday, 1992; Demanins & Hess, 1996) and do not strongly covary with spatial frequency (Demanins &

Hess, 1996). Perceptually, we would expect strabismic amblyopes to see a much less structured stimulus with their amblyopic visual system. Might this be the reason for their reduced brain activation? Positional uncertainty has been shown to disrupt contour integration of curved figures in normal subjects and to underlie the contour integration deficit in strabismic amblyopia (Hess *et al.* 1997). Furthermore, others have suggested that animals made surgically strabismic exhibit reduced temporal synchrony (Roelfsema *et al.* 1994) and as a consequence reduced contour integration (Singer & Gray, 1995). We measured fMRI activation in three normal subjects to a stimulus (Fig. 1*B* and *D*) that was a replica of the previous stimulus used but where the global contours were disrupted without any alteration to the local contrast, spatial frequency or orientation information. We could not find any evidence that disrupting the contour information in the stimulus used here reduced the V1 fMRI response in normal subjects. Thus the contour strength of the stimulus used did not underlie the fMRI activation in normal subjects and therefore an anomaly to contour integration *per se* in amblyopia is unlikely to provide a satisfactory explanation for the reduced cortical activation that we observed.

What is clear is that this reduced activation to high contrast stimuli well within the amblyopic passband involves area V1 as well as extra-striate areas, contrary to some recent reports (Imamura *et al.* 1997; Sireteanu *et al.* 1998). It may be similar to the abnormality revealed by optical imaging at low spatial frequencies in strabismic cats (Schmidt *et al.* 1999). Those authors speculated that the reduced V1 activity in strabismic cats was a reflection of anomalous intra-areal connectivity and/or impaired feedback from other visual areas which themselves may be anomalous. One aspect of visual processing that has been shown to depend on such lateral (Malach *et al.* 1993; Bosking *et al.* 1997) and feedback (Hupe *et al.* 1998) connections is contour integration. We did not find any evidence for reduced activation when the circular nature of the contours comprising the stimulus used here was disrupted, suggesting that, at least for our results, there may not be a large contribution from feature-binding mechanisms.

On the other hand, the reduced activation that we observed for the amblyopic cortex may be related to the loss of binocular cells in monkey cortex combined with an imbalance in the ocular dominance resulting in a greater proportion of cells being driven through the normal, fixing eye (Baker *et al.* 1974; Crawford & von Noorden, 1979; Eggers *et al.* 1984; Fenstemaker *et al.* 1997; Kiorpes *et al.* 1998). Though this is generally not found in most strabismic monkeys (Kiorpes *et al.* 1998), there is histological (Fenstemaker *et al.* 1997) and electrophysiological (Baker *et al.* 1974; Crawford & von Noorden, 1979) evidence that it may occur in severely amblyopic monkeys. The majority of the subjects in this study had severe

amblyopia and it remains to be determined whether their ocular dominance columns are very different in size. For this to explain our current results it would have to be shown that the reduction in ocular dominance columns in amblyopia covaries with peak spatial frequency response of cortical cells. Arguing against this explanation, a recent report suggests that the ocular dominance columns are of normal dimensions, at least in a strabismic human with severe amblyopia as the result of an accommodative esotropia (Horton & Hocking, 1996). It is hard to say what psychophysical impact such a deficit, if present, would have. The majority of the present psychophysics does not support an explanation based on undersampling for either the contrast sensitivity (Demanins *et al.* 1999) or positional losses in amblyopia (Hess & Field, 1994). Our current understanding of the neural basis of contrast sensitivity is based on the responses of cells tuned for spatial frequency, orientation, direction and contrast (Hawken & Parker, 1990) and not on their absolute number (Lashley, 1929). Unless the reduced activation by the amblyopic eye shows some selectivity, it is hard to understand how it could underlie the contrast sensitivity loss.

Site of the cortical deficit

Our results, specifically those using the large field stimulus (Fig. 6), indicate that V1 and other extra-striate areas show reduced levels of activation in amblyopia. This is suggestive of V1 being the earliest anomalous site in the pathway. This would be consistent with the animal neurophysiology literature for cat and monkey (Blakemore & Vital-Durand, 1986; Levitt *et al.* 1989; Crewther & Crewther, 1990). However, because of the abundance of feedback connections from extra-striate cortex onto V1, it remains a possibility that the lack of response from V1 is due to a primary abnormality in the extra-striate cortex. We used elementary stimuli to try to avoid such interactions which have been shown in figure/ground tasks in primates (Hupe *et al.* 1998) and we were unable to find, in normal subjects, any influence of contour-binding mechanisms for the stimulus used which may rely on such feedback.

Eccentric fixation

A number of the strabismic amblyopes we studied exhibited eccentric fixation (Table 1). This poses a potential problem for the interpretation of the results from the small field experiment in that activation due to stimulation in each eye will map to different regions of the retinotopic cortex. Is our analysis confounded by the possibility that the cortex driven by the amblyopic eye is normal but simply displaced? We do not feel that this is the case as neither of the measures of cortical activation we used were biased towards the fellow normal eye. The number of voxels measure, based purely on the amount of stimulus-correlated cortical activity (and therefore independent of cortical location), showed large differences

between normal fellow and amblyopic eye activation (Fig. 3). Similarly, the template used to form the measure of percentage BOLD change is based on an equally weighted average of the data from both eyes; therefore, if the amblyopic eye response were normal but displaced, the template would be larger and the average percentage BOLD change across this larger subset of voxels would be reduced equally for both eyes. Furthermore, during amblyopic eye stimulation one would expect to see hemispheric asymmetries in the amount of activated cortex that correlated with the degree of eccentric fixation. We found no correlation (rank correlation (R) = -0.046 for degree of eccentric fixation *vs.* number of active voxels in predicted hemisphere), although, as discussed in the next paragraph, we did find asymmetries. As clearly shown by the large field experiments, activation due to stimulation of the amblyopic eye was reduced throughout both hemispheres but this is not a consequence of eccentric fixation.

Previous reports have noted asymmetries in brain activation between the hemispheres of normal and amblyopic eyes. Demer and colleagues (see Demer, 1993) using PET found a greater level of activation in the contralateral hemisphere of both normal and amblyopic subjects. This is reflected in primate neurophysiology where the contralateral cortex drives 84% of cells in normal animals (Kiorpes *et al.* 1998). Imamura *et al.* (1997), also using PET, found the largest difference in activation to be localized to the hemisphere ipsilateral to the amblyopic eye. In general, consistent with recent primate neurophysiology (Kiorpes *et al.* 1998), we did not find consistent hemispheric differences in brain activation. For example, in 20 out of 38 cases more significant activity was found in the hemisphere ipsilateral to the stimulated eye. In 13 out of 19 cases, the amblyopic deficit (difference between the number of voxels active in a hemisphere when stimulated by the fixing and fellow amblyopic eyes) was greater in the hemisphere ipsilateral to the amblyopic eye.

ANDERSON, S. J., HOLLIDAY, I. E. & HARDING, G. F. A. (1999). Assessment of cortical dysfunction in human strabismic amblyopia using magnetoencephalography (MEG). *Vision Research* **39**, 1723–1738.

ARDEN, G. B. & BARNARD, W. B. (1979). Effect of occlusion on the visually evoked potential in amblyopia. *Transactions of the Ophthalmological Society, UK* **99**, 419–426.

BAKER, F. H., GRIGG, P. & VON NOORDEN, G. K. (1974). Effects of visual deprivation and strabismus on the response of neurons in the visual cortex of the monkey, including studies of striate and pre-striate cortex in normal animals. *Brain Research* **66**, 185–208.

BANDETTINI, P. A., JESMANOWICZ, A., WONG, E. C. & HYDE, J. S. (1993). Processing strategies for time-course data sets in functional MRI of the human brain. *Magnetic Resonance in Medicine* **30**, 161–173.

BEDELL, H. D. & FLOM, M. C. (1981). Monocular spatial distortion in strabismic amblyopia. *Investigative Ophthalmology and Visual Science* **20**, 263–268.

BEDELL, H. E. & FLOM, M. C. (1983). Normal and abnormal space perception. *American Journal of Optometry and Physiological Optics* **60**, 426–435.

BLAKEMORE, C. & VITAL-DURAND, F. (1986). Effects of visual deprivation on the development of the monkey's lateral geniculate nucleus. *Journal of Physiology* **380**, 493–511.

BOSKING, W. H., ZHANG, Y., SCHOFIELD, B. & FITZPATRICK, D. (1997). Orientation selectivity and the arrangement of horizontal connections in the tree shrew striate cortex. *Journal of Neuroscience* **17**, 2112–2127.

BOYNTON, G. M., ENGEL, S. A., GLOVER, G. H. & HEEGER, D. J. (1996). Linear systems analysis of fMRI in human V1. *Journal of Neuroscience* **16**, 4207–4221.

CHINO, Y. M., SHANSKY, M. S., JANKOWSKI, W. L. & BANSER, F. A. (1983). Effects of rearing kittens with convergent strabismus on development of receptive-field properties in striate cortex neurons. *Journal of Neurophysiology* **50**, 265–286.

COHEN, M. S. & DUBOIS, R. M. (1999). Stability, repeatability, and the expression of signal magnitude in functional magnetic resonance imaging. *Journal of Magnetic Resonance Imaging* **10**, 33–40.

COLLINS, D. L., NEELIN, P., PETERS, T. M. & EVANS, A. C. (1994). Automatic 3D intersubject registration of MR volumetric data in standardized Talairach space. *Journal of Computer Assisted Tomography* **18**, 192–205.

CRAWFORD, M. L. & VON NOORDEN, G. K. (1979). The effects of short-term experimental strabismus on the visual system in *Macaca mulatta*. *Investigative Ophthalmology and Visual Science* **18**, 496–505.

CREWETHER, D. P. & CREWETHER, S. G. (1990). Neural site of strabismic amblyopia in cats: spatial frequency deficit in primary cortical neurons. *Experimental Brain Research* **79**, 615–622.

DEMANINS, R. & HESS, R. F. (1996). Positional loss in strabismic amblyopia – interrelationship of alignment threshold, bias, spatial scale and eccentricity. *Vision Research* **36**, 2771–2794.

DEMANINS, R., WANG, Y.-Z. & HESS, R. F. (1999). The neural deficit in strabismic amblyopia: sampling considerations. *Vision Research* **39**, 3575–3585.

DEMER, J. L. (1993). Positron emission tomography studies of cortical function in human amblyopia. *Neuroscience and Biobehavioral Reviews* **17**, 469–476.

DEMER, J. L., VON NOORDEN, G. K., VOLKOW, N. D. & GOULD, K. L. (1988). Imaging of cerebral blood flow and metabolism in amblyopia by positron emission tomography. *American Journal of Ophthalmology* **105**, 337–347.

EGGERS, H. M., GIZZI, M. S. & MOVSHON, J. A. (1984). Spatial properties of striate cortical neurons in esotropic macaques. *Investigative Ophthalmology and Visual Science* **25** (suppl.), S278.

ENGEL, S. A., GLOVER, G. H. & WANDELL, B. A. (1997). Retinotopic organization in human visual cortex and the spatial precision of functional MRI. *Cerebral Cortex* **7**, 181–192.

ENGEL, S. A., RUMELHART, D. E., WANDELL, B. A., LEE, A. T., GLOVER, G. H., CHICHILNISKY, E. J. & SHADLEN, M. N. (1994). fMRI of human visual cortex. *Nature* **369**, 525.

FENSTEMAKER, S. B., GEORGE, K. H., KIORPES, L. & MOVSHON, J. A. (1997). Tangential organization of eye dominance in area V1 of macaques with strabismic amblyopia. *Society for Neuroscience Abstracts* **23**, 2363.

- GSTALDER, R. J. & GREEN, D. G. (1971). Laser interferometric acuity in amblyopia. *Journal of Pediatric Ophthalmology* **8**, 251–256.
- HARRAD, R. A. & HESS, R. F. (1992). Binocular integration of contrast information in amblyopia. *Vision Research* **32**, 2135–2150.
- HAWKEN, M. J. & PARKER, A. J. (1990). Detection and discrimination mechanisms in the striate cortex of the Old-World monkey. In *Vision Coding and Efficiency*, vol. 10, ed. BLAKEMORE, C., pp. 103–116. Cambridge University Press, UK.
- HESS, R. F. & BRADLEY, A. (1980). Contrast perception above threshold is only minimally impaired in human amblyopia. *Nature* **287**, 463–464.
- HESS, R. F., CAMPBELL, F. W. & GREENHALGH, T. (1978). On the nature of the neural abnormality in human amblyopia; neural aberrations and neural sensitivity loss. *Pflügers Archiv* **377**, 201–207.
- HESS, R. F., CAMPBELL, F. W. & ZIMMERN, R. (1980). Differences in the neural basis of human amblyopia: effect of mean luminance. *Vision Research* **20**, 295–305.
- HESS, R. F. & FIELD, D. J. (1994). Is the spatial deficit in strabismic amblyopia due to loss of cells or to an uncalibrated disarray of cells? *Vision Research* **34**, 3397–3406.
- HESS, R. F. & HOLLIDAY, I. E. (1992). The spatial localization deficit in amblyopia. *Vision Research* **32**, 1319–1339.
- HESS, R. F. & HOWELL, E. R. (1977). The threshold contrast sensitivity function in strabismic amblyopia: Evidence for a two type classification. *Vision Research* **17**, 1049–1055.
- HESS, R. F., MCILHAGGA, W. & FIELD, D. J. (1997). Contour integration in strabismic amblyopia: the sufficiency of an explanation based on positional uncertainty. *Vision Research* **37**, 3145–3161.
- HESS, R. F. & POINTER, J. S. (1985). Differences in the neural basis of human amblyopia: the distribution of the anomaly across the visual field. *Vision Research* **25**, 1577–1594.
- HORTON, J. C. & HOCKING, D. R. (1996). Pattern of ocular dominance columns in human striate cortex in strabismic amblyopia. *Visual Neuroscience* **13**, 787–795.
- HUPE, J. M., JAMES, A. C., PAYNE, B. R., LOMBER, S. G., GIRARD, P. & BULLIER, J. (1998). Cortical feedback improves discrimination between figure and background by V1, V2 and V3 neurons. *Nature* **394**, 784–787.
- IMAMURA, K., RICHTER, H., FISCHER, H., LENNERSTRAND, G., FRANZEN, O., RYDBERG, A., ANDERSSON, J., SCHNEIDER, H., ONOE, H., WATANABE, Y. & LANGSTROM, B. (1997). Reduced activity in the extrastriate visual cortex of individuals with strabismic amblyopia. *Neuroscience Letters* **225**, 173–176.
- KABASAKAL, L., DEVRANOGLU, K., ARSLAN, O., ERDIL, T. Y., SONMEZOGLU, K., USLU, I., TOLUN, H., ISITMAN, A. T., OZKER, K. & ONSEL, C. (1995). Brain SPECT evaluation of the visual cortex in amblyopia. *Journal of Nuclear Medicine* **36**, 1170–1174.
- KIOPES, L., KIPER, D. C., O'KEEFE, L. P., CAVANAUGH, J. R. & MOVSHON, J. A. (1998). Neuronal correlates of amblyopia in the visual cortex of macaque monkeys with experimental strabismus and anisometropia. *Journal of Neuroscience* **18**, 6411–6424.
- KUBOVA, Z., KUBA, M., JURAN, J. & BLAKEMORE, C. (1996). Is the motion system relatively spared in amblyopia? Evidence from cortical evoked potentials. *Vision Research* **36**, 181–190.
- LAGREZE, W.-D. & SIRETEANU, R. (1991). Two-dimensional spatial distortions in human strabismic amblyopia. *Vision Research* **31**, 1271–1288.
- LASHLEY, K. S. (1929). *Brain Mechanisms and Intelligence*. University of Chicago, Chicago, USA.
- LEVI, D. M. & KLEIN, S. A. (1983). Spatial localization in normal and amblyopic vision. *Vision Research* **23**, 1005–1017.
- LEVI, D. M. & KLEIN, S. A. (1985). Vernier acuity, crowding and amblyopia. *Vision Research* **25**, 979–991.
- LEVI, D. M. & NANNY, R. E. (1982). The pathophysiology of amblyopia: Electrophysiological studies. *Annals of the New York Academy of Sciences* **388**, 243–263.
- LEVI, M. & HARWERTH, R. S. (1977). Spatio-temporal interactions in anisometric and strabismic amblyopia. *Investigative Ophthalmology and Visual Science* **16**, 90–95.
- LEVITT, J. B., MOVSHON, J. A., SHERMAN, S. M. & SPEAR, P. D. (1989). Effects of monocular deprivation on macaque LGN. *Investigative Ophthalmology and Visual Science* **30** (suppl.), S296.
- MAES, F., COLLIGNON, A., VANDERMEULEN, D., MARCHAL, G. & SUETENS, P. (1997). Multimodality image registration by maximization of mutual information. *IEEE Transactions on Medical Imaging* **16**, 187–198.
- MALACH, R., AMIR, Y., HAREL, M. & GRINVALD, A. (1993). Relationship between intrinsic connections and functional architecture revealed by optical imaging and in vivo targeted biocytin injections in primate striate cortex. *Proceedings of the National Academy of Sciences of the USA* **90**, 10469–10473.
- PRESS, W. H., TEUKOLSKY, S. A., VETTERLING, W. T. & FLANNERY, B. P. (1992). *Numerical Recipes in C: The Art of Scientific Computing*. Cambridge University Press, Cambridge, UK.
- ROELFSEMA, P. R., KONIG, P., ENGEL, A. K., SIRETEANU, R. & SINGER, W. (1994). Reduced synchronization in the visual cortex of cats with strabismic amblyopia. *European Journal of Neuroscience* **6**, 1645–1655.
- SCHMIDT, K. E., GALUSKE, R. A. W. & SINGER, W. (1999). Deficits of functional processing in V1 of esotropic cats as revealed by optical imaging. *Investigative Ophthalmology and Visual Science* **40** (suppl.), S644.
- SERENO, M. I., DALE, A. M., REPPAS, J. B., KWONG, K. K., BELLIVEAU, J. W., BRADY, T. J., ROSEN, B. R. & TOOTELL, R. B. (1995). Borders of multiple visual areas in humans revealed by functional magnetic resonance imaging. *Science* **268**, 889–893.
- SINGER, W. & GRAY, C. M. (1995). Visual feature integration and the temporal synchronization hypothesis. *Annual Review of Neuroscience* **18**, 555–586.
- SIRETEANU, R., LAGREZE, W.-D. & CONSTANTINESCU, D. H. (1993). Distortions in two-dimensional visual space perception in strabismic observers. *Vision Research* **33**, 677–690.
- SIRETEANU, R., TONHAUSEN, N., MICKLI, L., LANFERMANN, H., ZANELLA, F. F. & SINGER, W. (1998). Cortical site of amblyopic deficit in strabismic and anisometric subjects. *Investigative Ophthalmology and Visual Science* **39** (suppl.), S909.
- SLED, J. G., ZIJDENBOS, A. P. & EVANS, A. C. (1998). A non-parametric method for automatic correction of intensity non-uniformity in MRI data. *IEEE Transactions on Medical Imaging* **17**, 87–97.
- SMITH, A. T., GREENLEE, M. W., SINGH, K. D., KRAEMER, F. M. & HENNING, J. (1998). The processing of first- and second-order motion in human visual cortex assessed by functional magnetic resonance imaging (fMRI). *Journal of Neuroscience* **18**, 3816–3830.
- TALAIRACH, J. & TOURNOUX, P. (1988). *Co-planar Stereotaxic Atlas of the Human Brain*. Thieme, New York.

- TEO, P. C., SAPIRO, G. & WANDELL, B. A. (1997). Creating connected representations of cortical gray matter for functional MRI visualization. *IEEE Transactions on Medical Imaging* **16**, 852–863.
- TOOTELL, R. B. H., MENDOLA, J. D., HADHIKHANI, N. K., LEDDEN, P. J., LIU, A. K., REPPAS, J. B., SERENO, M. I. & DALE, A. M. (1997). Functional analysis of V3A and related areas in human visual cortex. *Journal of Neuroscience*, **17**, 7060–7078.
- WOODS, R. P., GRAFTON, S. T., HOLMES, C. J., CHERRY, S. R. & MAZZIOTTA, J. C. (1998). Automated image registration: I. General methods and intrasubject, intramodality validation. *Journal of Computer Assisted Tomography* **22**, 141–154.

Acknowledgements

This work was supported by a Canadian MRC grant (Mt10818) to R. F. H. We are grateful to V. Petre, R. Hoge, C. B. Williams and A. Evans for their help.

Corresponding author

R. F. Hess: McGill Vision Research, 687 Pine Avenue W. (H4-14), Montreal, PQ, Canada H3A 1A1.

Email: rhess@vision.mcgill.ca